NASA TECHNICAL NOTE

NASA TN D-7608

NASA TN D-7608

TWO-DIMENSIONAL ANALYSIS OF HEAT AND MASS TRANSFER IN POROUS MEDIA USING THE STRONGLY IMPLICIT PROCEDURE

by Donald M. Curry

Lyndon B. Johnson Space Center
Houston, Texas 77058

NATIONAL AERONAUTICS AND SPACE ADMINISTRATION • WASHINGTON, D. C. • MARCH 1974

1. Report No.	2. Government Accession No.	3. Recipient's Catalog No.
NASA TN D-7608		

4. Title and Subtitle	5. Report Date
TWO-DIMENSIONAL ANALYSIS OF HEAT AND MASS TRANSFER IN POROUS MEDIA USING THE STRONGLY IMPLICIT PROCEDURE	March 1974
	6. Performing Organization Code
7. Author(s)	8. Performing Organization Report No.
Donald M. Curry, JSC	JSC S-382
	10. Work Unit No.
9. Performing Organization Name and Address	986-15-31-04-72
Lyndon B. Johnson Space Center Houston, Texas 77058	11. Contract or Grant No.
	13. Type of Report and Period Covered
12. Sponsoring Agency Name and Address	Technical Note
National Aeronautics and Space Administration Washington, D.C. 20546	14. Sponsoring Agency Code

15. Supplementary Notes

16. Abstract

Numerical results of the heat and mass transfer in a porous matrix are presented. The coupled, nonlinear partial differential equations describing this physical phenomenon are solved in finite difference form for two dimensions, using a new iterative technique (the strongly implicit procedure). The influence of the external environment conditions (heating and pressure) is shown to produce two-dimensional flow in the porous matrix. Typical fluid and solid temperature distributions in the porous matrix and internal pressure distributions are presented.

17. Key Words (Suggested by Author(s))	18. Distribution Statement
Porous Materials; Ablation; Momentum Equations; Energy Equations; Convection; Conduction	Subject Category 33

19. Security Classif. (of this report)	20. Security Classif. (of this page)	21. No. of Pages	22. Price
None	None	36	$3.00

*For sale by the National Technical Information Service, Springfield, Virginia 22151

CONTENTS

TABLE

FIGURES

TWO-DIMENSIONAL ANALYSIS OF HEAT AND MASS TRANSFER IN POROUS MEDIA USING THE STRONGLY IMPLICIT PROCEDURE

By Donald M. Curry
Lyndon B. Johnson Space Center

SUMMARY

The conservation relations describing the transient heat and mass transfer in a porous matrix are coupled, nonlinear partial differential equations. The equations are solved in finite difference form by using a recently developed numerical technique (the strongly implicit procedure). The application of the procedure is discussed. Sample numerical results demonstrate the two-dimensional characteristics of heat and mass transfer in a porous matrix. By imposing external pressure distributions, external heat flux distributions, and backface mass flux injection distributions, the effects on the internal pressure distributions, the internal mass flow rates, and the internal temperature distributions are obtained.

INTRODUCTION

An understanding of heat transfer and fluid flow in porous media is important in many engineering fields, such as soil mechanics, powder metallurgy, chemical processing, and petroleum reservoir recovery. The successful application of ablation materials or transpiration cooling systems to protect ballistic missiles and manned spacecraft has motivated investigations of the heat- and mass-transfer processes occurring in a porous matrix at high temperatures. The basic thermal features of an ablative system are a high surface temperature, a steep temperature gradient within the material, and the transpiration of gases (generated by thermal decomposition) through a high-temperature porous matrix. The high surface temperature permits approximately 80 percent of the external heat flux to be reradiated by the surface. The steep temperature gradient permits a cool backface with a hot external surface. The transpiring gases remove some heat being conducted into the material and also thicken the boundary layer, thereby decreasing the convective heating to the wall.

Both ground-based and flight test data (obtained from a charring ablator used on the Apollo spacecraft) have indicated a need to extend the currently available analytical techniques to describe more completely and to predict the expected performance of the thermal protection system. An analysis of the thermal response of the Apollo ablative heat shield (ref. 1) has shown a discrepancy in current design methods for calculating surface recession. The prediction of the one-dimensional analytical model (ref. 1) compares favorably with flight data but underestimates the surface recession results in ground-based tests. Improvement of the prediction technique requires further study of phenomena associated with aerothermodynamic environment, material chemistry, and multidimensional heat and mass transfer in a porous char matrix. This report considers only two-dimensional heat and mass transfer in a porous material. An analysis by Bush and Dow (ref. 2) of the pressure fields within cylindrical and hemispherical ablative chars under steady-state conditions has indicated that the gas flow through the char can be significantly different from that predicted on the basis of a one-dimensional model. The theoretical results further indicated the possibility of an influx of boundary-layer gas into the char. However, Bush and Dow considered no coupling of the energy and momentum equations in the analysis.

Heretofore, analytical and experimental studies in the literature are generally not concerned with the coupled heat-transfer/fluid-flow problems that occur in the chemical, petroleum, and aerospace industries. However, Bland (ref. 3) showed the existence of coupling between the momentum and energy relationships when the steady-state, Darcy continuity equation was used to describe the flow of a gas through a porous medium. Bland considered a temperature difference between the gas and solid and heat conduction in the solid but neglected the gas heat conduction and storage in the fluid energy equation. The coupled equations are developed for the case of three independent space variables and one time variable. The theoretical treatment of Bland shows clearly the coupling of the momentum and energy equations used to describe simultaneous heat transfer and fluid flow in a porous matrix.

More recently, Schneider et al. (ref. 4) performed a two-dimensional, steady-state analysis of an active transpiration cooling system. For an incompressible coolant flow through a porous nose tip, the two-dimensional solution was found to be important in assessing the internal coolant distribution and in determining the driving pressure required to prevent coolant starvation at the nose tip. For the purpose of comparison, Schneider et al. performed a one-dimensional analysis that resulted in a nonconservative design with respect to expulsion system pressure requirements.

Del Casal (ref. 5) investigated the effects of multidimensional flow on heat transfer for the stagnation region of blunt axisymmetric surfaces. The internal-flow solutions were coupled with those of the external boundary layer by matching solutions at the outer surface of the porous matrix. Although only steady-state solutions were performed, Del Casal included the effects of inertia in the momentum equation; these had been neglected by Schneider et al.

Pittman and Howser (ref. 6) analyzed the transient response of an axisymmetric charring ablator, considering internal flow. They assumed thermal equilibrium between the gas and solid phases. Surface recession and pyrolysis interface rates were shown to be affected by multidimensional flow of the pyrolysis gases through the char layer.

Numerous analytical models for predicting pressure distribution, mass flow rate, and thermal response of porous materials are published for a wide variety of boundary conditions. One predominant assumption in a majority of these analyses is the independence of the energy and momentum conservation relations used for performance predictions. Voluminous material is available on both heat transfer and pressure-drop flow studies for a porous matrix. However, the use of porous materials in spacecraft thermal protection systems has emphasized the importance of understanding the more complex, coupled relationship. The general lack of available solutions that consider the coupled energy and momentum relations used in describing the thermal response of a transpiration cooling system motivated this study.

SYMBOLS

A, B, C, D, E, G, H, Q	parameters known from previous time level and previous iteration
AX, AY	functions defined in equation (B3)
b, c, d, e, f	coefficients defined in equation (21)
C_p	specific heat
g	gravitational constant
h_v	volumetric heat-transfer coefficient
K	proportionality factor
k	thermal conductivity
k_x, k_y	thermal conductivity in x and y directions, respectively
L_x, L_y	length in x and y directions, respectively
$\dot{m}$	mass flow rate, $\rho\vec{V}$
m'''	volume source term
npx	total number of nodes in x direction
npy	total number of nodes in y direction
P	pressure
$\dot{q}$	convective heating rate
q'''	volumetric heat source (or sink)
R	universal gas constant
T	temperature

T_{eq}	radiation equilibrium temperature
T_i	initial temperature
T'	unknown temperature in difference equations
t	time
$\hat{U}$	total internal energy
u	velocity in x direction
$\vec{V}$	superficial velocity
$V_{i,j}$	intermediate coefficient used in the solution algorithm
v	velocity in y direction
$\vec{v}$	velocity in a pore
x,y	space coordinates
α	viscous coefficient
β	inertial coefficient
γ	iteration parameter
δ	dependent-variable difference between the new time step or iteration and the previous time step or iteration
ϵ	emissivity
μ	viscosity
ρ	density
σ	Stefan-Boltzmann constant
τ	viscous stress tensor
Φ	viscous dissipation
ϕ	porosity, ratio of void area to total area
ψ	convective heat-blocking ratio due to mass injection

Subscripts:

e	external
f	fluid
i	x-direction node location
j	y-direction node location
o	without blockage
Ref	reference
Stag	stagnation
s	solid
w	matrix surface

Superscript:

n	iteration or time step

Operators:

(')	indicates parameter at next time step
∇	differential operator

THEORETICAL RELATIONS

The unsteady heat transfer of a compressible gas flowing within a porous matrix can be described by the solution of the conservation equations for mass, momentum, and energy. The fundamental assumption is the use of a continuum model for the porous matrix. Briefly, the volume element used in deriving the conservation equations is assumed large with respect to the individual pores so that the flow field may be considered a continuum. The application of the conservation equations for mass, momentum, and energy to the unsteady flow of a gas, with heat transfer, through a porous matrix is presented in appendix A.

For the case of a two-dimensional heat transfer and fluid flow in a porous medium, the governing differential relations can be written as follows. The Darcy continuity equation is

$$\frac{\phi}{P}\frac{\partial}{\partial t}\left(\frac{P^2}{T_f}\right) - \frac{\partial}{\partial x}\left[\frac{1}{T_f(\alpha\mu + \beta\rho|u|)}\frac{\partial P^2}{\partial x}\right] - \frac{\partial}{\partial y}\left[\frac{1}{T_f(\alpha\mu + \beta\rho|v|)}\frac{\partial P^2}{\partial y}\right] = 2Rm''' \tag{1}$$

where ϕ = porosity

P = pressure

t = time

T = temperature

x, y = space coordinates

α = viscous coefficient

μ = viscosity

β = inertial coefficient

ρ = density

u = velocity in x direction

v = velocity in y direction

R = universal gas constant

m''' = volume source term

The energy considerations when T_{fluid} is not equal to T_{solid} are as follows. The fluid energy equation is

$$C_{p_f}\rho_f\left(\frac{\partial T_f}{\partial t} + u\frac{\partial T_f}{\partial x} + v\frac{\partial T_f}{\partial y}\right) - \left(\frac{\partial P}{\partial t} + u\frac{\partial P}{\partial x} + v\frac{\partial P}{\partial y}\right) + \left[C_{p_f}T_f + \frac{1}{2}\left(u^2 + v^2\right)\right]m'''$$

$$= \frac{\partial}{\partial x}\left(k_f\frac{\partial T_f}{\partial x}\right) + \frac{\partial}{\partial y}\left(k_f\frac{\partial T_f}{\partial y}\right) + \frac{h_v}{\phi}\left(T_s - T_f\right) + q''' \tag{2}$$

where C_p = specific heat

k = thermal conductivity

h_v = volumetric heat-transfer coefficient

q''' = volumetric heat source (or sink)

The solid energy equation is

$$\rho_s C_{p_s} \frac{\partial T_s}{\partial t} = \frac{\partial}{\partial x}\left(k_s \frac{\partial T_s}{\partial x}\right) + \frac{\partial}{\partial y}\left(k_s \frac{\partial T_s}{\partial y}\right) - \frac{h_v}{(1 - \phi)}\left(T_s - T_f\right) + q''' \tag{3}$$

These three partial differential equations plus two algebraic relations, the Darcy pressure drop (eq. (A11)) and the perfect gas equation of state (eq. (A12)), form the complete set of equations.

BOUNDARY AND INITIAL CONDITIONS

The following specification of boundary and initial conditions is an important phase in describing the physical system being modeled. In the present analyses, the physical domain consists of a rectangular matrix with dimensions L_x and L_y as shown in figure 1. When these analyses are applied to the case of a charring ablator, the ablator exterior surface is represented by the plane $x = 0$ and the char thickness is L_x. The fluid enters the matrix at the rear face $x = L_x$. The mass flow rate at the center rear face $\dot{m}(L_x, 0)$ is used as the base value to nondimensionalize local mass flow rates. All injected gases flow toward the heated surface $x = 0$; no flow reversal is permitted. Mathematically, the boundary conditions for the matrix and fluid energy equation at the exterior surface are

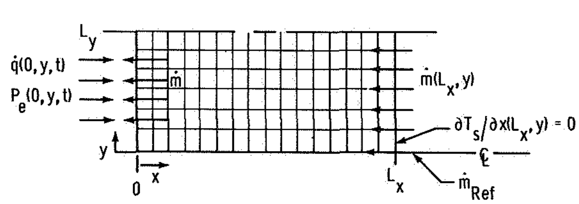

Figure 1. - Two-dimensional porous matrix.

$$x = 0; \qquad -k_s \frac{\partial T_s}{\partial x} = \dot{q}_{net} = \psi \dot{q}_o - \sigma \epsilon T_s^{\,4} \tag{4}$$

$$\frac{\partial^2 T_f}{\partial x^2} = 0 \tag{5}$$

where $\dot{q}$ = convective heating rate

σ = Stefan-Boltzmann constant

ϵ = emissivity

The net heat at the exterior surface is specified by equation (4). Here, ψ is defined as the ratio of the convective heat flux with blowing to the convective heat flux that would exist without mass injection. For the boundary condition as shown by equation (5), the matrix surface does not require that fluid and matrix temperatures be equal; it does not preclude $T_s = T_f$. This boundary condition permits conduction in the fluid at the fluid exit.

The temperatures of the gas and solid are assumed to be equal along the injection plane. This is consistent with the gas being formed at a local solid decomposition temperature.

$$x = L_x; \qquad T_f = T_s \tag{6}$$

A thermally adiabatic back surface exists along the plane of mass injection.

$$x = L_x; \qquad \frac{\partial T_s}{\partial x} = 0 \tag{7}$$

Symmetric boundaries are assumed in the y direction.

$$y = 0, L_y; \qquad \frac{\partial T_f}{\partial y} = 0, \quad \frac{\partial T_s}{\partial y} = 0 \tag{8}$$

The unsteady boundary conditions on the momentum equation permit a variable pressure in the y direction.

$$x = 0; \qquad P(0,y,t) = P_e(y,t) \tag{9}$$

$$x = L_x; \qquad \frac{\partial P}{\partial x} = 0 \tag{10}$$

where P_e is external pressure. The boundary condition illustrated by equation (10) does not permit flow reversal at the injection plane. This is a reasonable assumption since an impermeable seal exists a small distance from the injection zone. Along the y boundary

$$y = 0; \qquad \frac{\partial P}{\partial y} = 0 \tag{11}$$

$$y = L_y; \qquad \frac{\partial P}{\partial y} = 0 \tag{12}$$

The initial pressure distribution is assumed constant and equal to the local external pressure at the start of the transient solution. No flow can occur in the y direction along the $x = L_x$ boundary, with symmetrical flow assumed at the boundaries for $y = 0$, $y = L_y$.

Equations (1), (2), and (3) describe the flow and heat transfer in a porous matrix and are coupled, nonlinear partial differential equations. The solution is achieved by approximating the partial derivatives by use of suitable finite difference expressions involving the independent and dependent variables. This procedure leads to a set of algebraic equations in the dependent variable from which the final value can be determined. Three basic finite difference formulas (forward, backward, and central difference) can be used to obtain the necessary relations. Once the finite differencing method has been chosen, a variety of solution techniques is available, each of which has its own peculiar advantages and limitations. For example, an explicit technique may require small integration time steps to ensure stability; the implicit technique seemingly does not have a time-step limitation but may require the solution of a large algebraic matrix.

In this investigation, an implicit central-difference numerical technique is used to obtain solutions for the momentum, energy, and continuity relations; it requires evaluation of the coefficients of the dependent variable at the previous time level and/or iteration as well as the solution of a set of linear difference equations for the dependent variables.

IMPLICIT DIFFERENCE EQUATION FORMULATION

A general two-dimensional region with an x-y grid system imposed is shown in figure 2. The implicit difference formulation used to solve equations (1), (2), and (3) can be illustrated conceptually

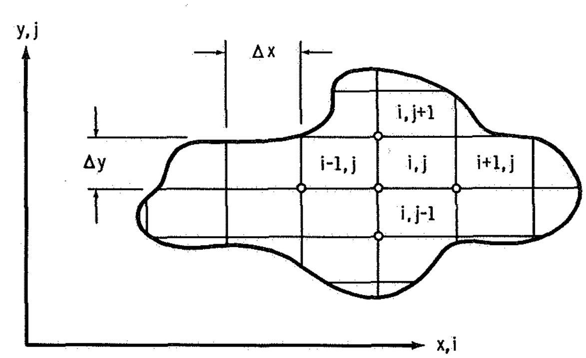

Figure 2. - Two-dimensional region with rectangular grid.

by consideration of the simpler problem of pure conduction. The transient heat conduction equation for this two-dimensional region is

$$\rho C_p \frac{\partial T}{\partial t} = \frac{\partial}{\partial x}\left(k_x \frac{\partial T}{\partial x}\right) + \frac{\partial}{\partial y}\left(k_y \frac{\partial T}{\partial y}\right) \tag{13}$$

An implicit finite difference equation for each grid point (i, j) within the specified region can be written as

$$\rho C_p\left(\frac{T'_{i,j} - T_{i,j}}{\Delta t}\right) = k_{x_{i,j}}\left[\frac{T'_{i+1,j} - 2T'_{i,j} + T'_{i-1,j}}{(\Delta x)^2}\right] + k_{y_{i,j}}\left[\frac{T'_{i,j+1} - 2T'_{i,j} + T'_{i,j-1}}{(\Delta y)^2}\right] \tag{14}$$

where, for the purposes of this illustration, k_x and k_y have been considered constant. The prime on each temperature represents an unknown temperature. Equation (14) can be written as

$$\left[\frac{k_{y_{i,j}}}{(\Delta y)^2}\right]T'_{i,j-1} + \left[\frac{k_{x_{i,j}}}{(\Delta x)^2}\right]T'_{i-1,j} - \left[\frac{\rho C_p}{\Delta t} + \frac{2k_{x_{i,j}}}{(\Delta x)^2} + \frac{2k_{y_{i,j}}}{(\Delta y)^2}\right]T'_{i,j}$$
$$+ \left[\frac{k_{x_{i,j}}}{(\Delta x)^2}\right]T'_{i+1,j} + \left[\frac{k_{y_{i,j}}}{(\Delta y)^2}\right]T'_{i,j+1} = -\frac{\rho C_p}{\Delta t} T_{i,j} \tag{15}$$

Rewriting equation (15) yields

$$AT'_{i,j-1} + BT'_{i-1,j} + CT'_{i,j} + DT'_{i+1,j} + ET'_{i,j+1} = Q_{i,j} \tag{16}$$

Equation (16) has five unknown temperatures per grid point (i,j). The values of A, B, C, D, E, and Q are known based on the previous time level and previous iteration. A set of equations similar to equation (16) can be written for all (i,j) grid points within the region and on the boundaries. This matrix of equations then can be inverted to yield the unknowns $T'_{i,j}$. For large systems of equations, this matrix solution can become very time consuming.

The development of the alternating direct implicit (ADI) method for the two-dimensional system proposed by Peaceman and Rachford (ref. 7) reduced the number of unknowns to three, as obtained for simple one-dimensional problems. Basically, the ADI solves the equations in one direction while assuming the dependent variable in the second dimension to be constant over the time interval. As an example, consider equation (16) for the first time step, in the x direction.

$$BT'_{i-1,j} + CT'_{i,j} + DT'_{i+1,j} = Q_{i,j} - AT_{i,j-1} - ET_{i,j+1} \tag{17}$$

The temperatures $T_{i,j-1}$ and $T_{i,j+1}$ are known from the previous time step. Equation (17) yields a tridiagonal matrix.

$$\begin{aligned}
&B_1T_{1,j} + C_1T_{2,j} && = Q_{1,j} \\
&A_2T_{1,j} + B_2T_{2,j} + C_2T_{3,j} && = Q_{2,j} \\
&\qquad A_3T_{2,j} + B_3T_{3,j} + C_3T_{4,j} && = Q_{3,j} \\
&\qquad\qquad A_{N-1}T_{N-2,j} + B_{N-1}T_{N-1,j} + C_{N-1}T_{N,j} && = Q_{N-1,j} \\
&\qquad\qquad\qquad A_NT_{N-1,j} + B_NT_{N,j} && = Q_{N,j}
\end{aligned} \tag{18}$$

Equation (18) is solved for the unknown temperatures by Gaussian reduction. Then, for the second time step, writing equation (16) in the y direction yields

$$AT'_{i,j-1} + CT'_{i,j} + ET'_{i,j+1} = Q_{i,j} - BT_{i-1,j} - DT_{i+1,j} \tag{19}$$

Once again, a tridiagonal matrix as shown by equation (18) is obtained. The advantages of solving a tridiagonal matrix over the matrix generated by equation (16) are apparent. The ADI method is not used in this study; rather, the strongly implicit procedure (SIP) is used in the next section.

STRONGLY IMPLICIT PROCEDURE

Recently, Stone (ref. 8) developed a new iterative method for solving sets of algebraic equations that occur for multidimensional systems. This method is known as the strongly implicit procedure and has been used successfully in solving the two-dimensional, steady-state heat conduction problem as well as multidimensional flow in a petroleum reservoir. The foundation of the SIP calculation method lies in the approximate factoring of the five-diagonal matrix (five nonzero elements in each row of matrix) generated by equation (16) into three-diagonal upper and lower triangular matrices. The detailed mathematical matrix reduction process, required to derive the upper and lower triangular matrices, is presented by Stone (ref. 8) and more recently by Bozeman (ref. 9).

The process of defining the upper and lower matrices involves the temperatures of the grid point (i,j). As shown in figure 3, the modified matrix equation involves not only the grid points indicated by the solid circles but also the temperatures at grid points $(i-1,j+1)$ and $(i+1,j-1)$ shown by the open circles.

The influence of these new temperatures in the modified equation is balanced partially by subtracting approximately equal terms. The modified equation for the unknown side of equation (16) becomes

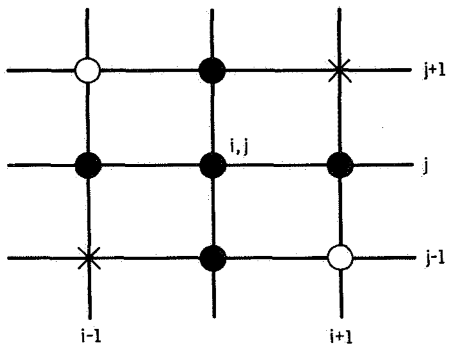

Figure 3. - Grid model for definition of upper and lower matrices.

$$\begin{aligned} &A_{i,j}T'_{i,j-1} + B_{i,j}T'_{i-1,j} + C_{i,j}T'_{i,j} \\ &+ D_{i,j}T'_{i+1,j} + E_{i,j}T'_{i,j+1} + H_{i,j}\Big[T'_{i+1,j-1} \\ &- \gamma\left(-T'_{i,j} + T'_{i+1,j} + T'_{i,j-1}\right)\Big] \\ &+ G_{i,j}\Big[T'_{i-1,j+1} - \gamma\left(-T'_{i,j} + T'_{i,j+1} + T'_{i-1,j}\right)\Big] \\ &= Q_{i,j} \end{aligned} \tag{20}$$

where γ is the iteration parameter. The first five terms are simply the original left side of equation (16), and the $H_{i,j}$, $G_{i,j}$ are used to cancel partially the temperatures at $(i-1,j+1)$ and $(i+1,j-1)$.

The equations used in this algorithm for SIP are

$$b_{i,j} = \frac{A_{i,j}}{1 + \gamma e_{i,j-1}} \tag{21a}$$

$$c_{i,j} = \frac{B_{i,j}}{1 + \gamma f_{i-1,j}} \tag{21b}$$

$$H_{i,j} = b_{i,j}e_{i,j-1} \tag{21c}$$

$$G_{i,j} = c_{i,j}f_{i-1,j} \tag{21d}$$

$$d_{i,j} = C_{i,j} + \gamma H_{i,j} + \gamma G_{i,j} - b_{i,j} f_{i,j-1} - c_{i,j} e_{i-1,j} \tag{21e}$$

$$e_{i,j} = \frac{D_{i,j} - \gamma H_{i,j}}{d_{i,j}} \tag{21f}$$

$$f_{i,j} = \frac{E_{i,j} - \gamma G_{i,j}}{d_{i,j}} \tag{21g}$$

and

$$R^n_{i,j} = Q_{i,j} - \left(A_{i,j} T^n_{i,j-1} + B_{i,j} T^n_{i-1,j} + C_{i,j} T^n_{i,j} + D_{i,j} T^n_{i+1,j} + E_{i,j} T^n_{i,j+1}\right) \tag{22}$$

where the exponent n is the iteration or time step. After solving for the coefficients b, c, d, e, and f, then all the intermediate coefficient values of $V_{i,j}$ are solved by

$$b_{i,j} V_{i,j-1} + c_{i,j} V_{i-1,j} + d_{i,j} V_{i,j} = R^n_{i,j} \tag{23}$$

Equations (21), (22), and (23) constitute the algorithm to be solved for the unknown variable $T^{n+1}_{i,j}$. These equations are valid for all points within the grid system. The following conditions, which must be satisfied for these equations on the boundaries, are illustrated in figure 4.

The coefficients generated by equations (21), (22), and (23) are intermediate coefficients used during the elimination process. The $V_{i,j}$ quantities are computed from equations (21), (22), and (23) by starting at the line $j = 1$ and letting i take on values from $1, 2, 3 \ldots$ npx nodes. Then j is incremented by 1 and the process is repeated.

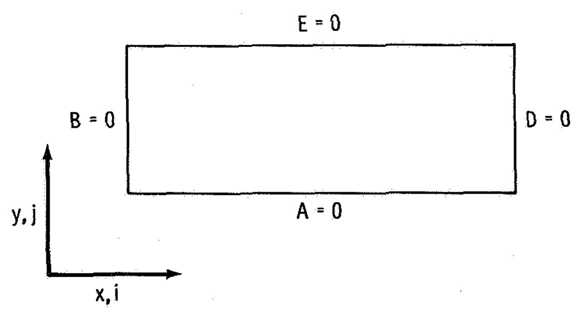

$A_{i,0}; E_{i,npy} = 0$ for $y = 0, y = L_y$

$B_{0,j}; D_{npx,j} = 0$ for $x = 0, x = L_x$

Figure 4. - Illustration of boundary condition restrictions.

After all $V_{i,j}$ coefficients have been generated and stored, equation (24) is solved for $\delta_{i,j}^{n+1}$ by simply reversing the order; that is, starting with $i = npx$ and $j = npy$.

$$\delta_{i,j}^{n+1} = V_{i,j} - e_{i,j}\delta_{i+1,j}^{n+1} - f_{i,j}\delta_{i,j+1}^{n+1} \tag{24}$$

where $\delta^{n+1} = T^{n+1} - T^{n}$

n = iteration or time step

$\therefore T^{n+1} \equiv T'$

Therefore, the values of temperature at the new time level $(n+1)$ can be calculated from a knowledge of T at the current time level (n). Stone (ref. 8) recommends a variation of the procedure by carrying out the calculation just described in reverse order on each alternate time step. This has the effect of using the temperatures $T_{i-1,j+1}$ and $T_{i+1,j-1}$ on the odd steps.

The value of the iteration parameter γ lies between 0 and 1. The minimum value is not critical and could be zero; however, Stone states that the maximum value can be critical for obtaining convergence. For a heat conduction problem with constant properties, Stone recommends

$$\gamma_{max} = 1 - \min\left[\frac{2(\Delta x)^2}{1 + \dfrac{k_y(\Delta x)^2}{k_x(\Delta y)^2}}, \frac{2(\Delta y)^2}{1 + \dfrac{k_x(\Delta y)^2}{k_y(\Delta x)^2}}\right] \tag{25}$$

It should be pointed out that equation (25) is for a particular problem, and it may be necessary to vary γ for other types of problems to determine its effect. In this work, a constant γ value of 0.95 was used successfully. The SIP formulation as applied to a simplified form of the fluid energy equation (2) is presented in appendix B.

SOLUTION TECHNIQUE

The two-dimensional nonlinear conservation equations (1), (2), and (3) were approximated by a set of finite difference equations compatible with Stone's algorithm. These equations are linearized by holding the nonlinear coefficients constant for each iterative calculation. The coefficients are then updated after each iteration. This set of linear equations is solved by application of equations (21) to (24). Because the equations are coupled through the nonlinear coefficients, the following iterative scheme was used as shown in figure 5.

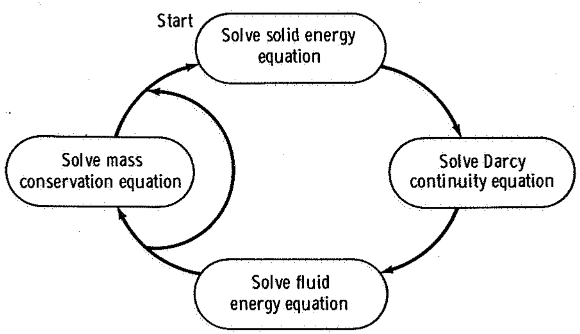

Figure 5. - Numerical iteration procedure.

The procedure is (1) to solve the solid energy equation by using the previous level values for flow rates, temperature, and physical properties; (2) to solve the Darcy continuity equation to obtain new pressures and velocities; (3) to obtain the fluid energy equation solution by using these latest values for flow rate, pressure, and temperature to obtain new fluid temperatures; and (4) to perform an independent calculation of the continuity equation (eq. (A1)) to ensure mass conservation. Three iterations per time step normally were required to obtain a satisfactory mass balance. The largest error occurs at the surface node where the pressure is being specified. Gas density for this node is evaluated from the continuity equation instead of the perfect gas law.

NUMERICAL RESULTS

The solution is capable of describing a wide variety of physical situations; however, only a limited number of representative cases are presented. More complete parametric comparisons for the porous matrix are provided in reference 10. Numerical results are provided for cases similar to those experienced by the Apollo configuration. The external pressure distribution, the external heat flux distribution, and the backface mass flux injection distribution are shown in dimensionless form in figure 6. The external distributions (mass flux injection at the rear boundary $x = L_x$, pressure and heat flux at the external boundary $x = 0$) were not time dependent in the cases under discussion. To identify the flow characteristics in the porous media, the decoupled solution (isothermal solution) is considered first. The effects of heat transfer on the internal flow characteristics are then considered by solving the coupled, two-dimensional equations.

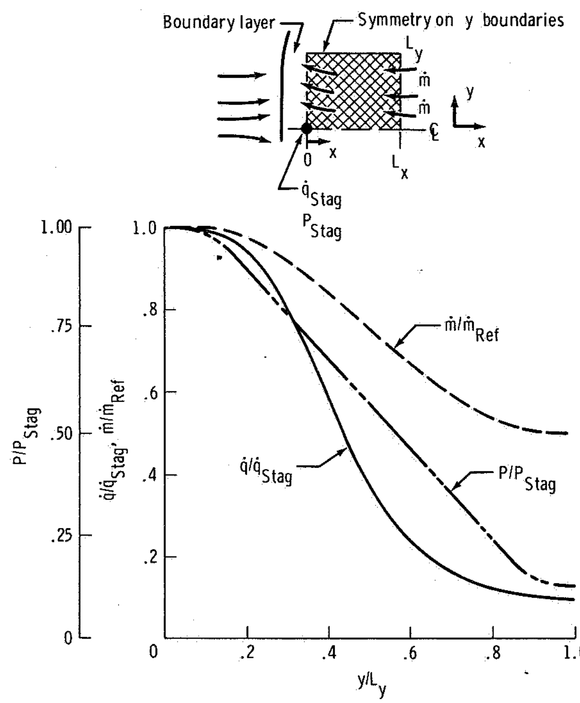

Figure 6. - External pressure gradient, heat flux, and mass injection flux ratios used to simulate typical Apollo conditions; where $P_{Stag} = P(0,0)$, $\dot{q}_{Stag} = \dot{q}(0,0)$, and $\dot{m}_{Ref} = \dot{m}(L_x,0)$.

Isothermal Solutions

A metallic matrix material is considered for examples of isothermal solutions. For the metallic matrix, the porosity ϕ is 0.42, the viscous coefficient α is 1.619×10^{10} m^{-2}, and the inertial coefficient β is 1.634×10^{4} m^{-1}.

If the Darcy continuity equation (eq. (1)) is solved for an isothermal case, the effect of the external pressure field on the internal flow in the matrix is demonstrated. An external pressure distribution (fig. 6) and a temperature of 556 K were used in the isothermal solution. A constant, uniform mass flux input at the rear surface was used. Air was used as the fluid flowing through the metallic matrix material and ablative char matrices; the corresponding properties of air were obtained from Kreith (ref. 11).

Based on an external stagnation pressure of 2.03×10^{3} N/m^{2}, the local mass flow-rate distribution in the x direction is shown in figure 7. The mass flow rate has been normalized by dividing by the mass injection at the backface $\dot{m}_{Ref} = \dot{m}(L_x, 0)$. Because the dimensionless mass flow rate does not vary substantially from unity, the internal flow is essentially one dimensional, indicating little effect of the external pressure distribution. The internal pressure distribution in the matrix is shown in figure 8.

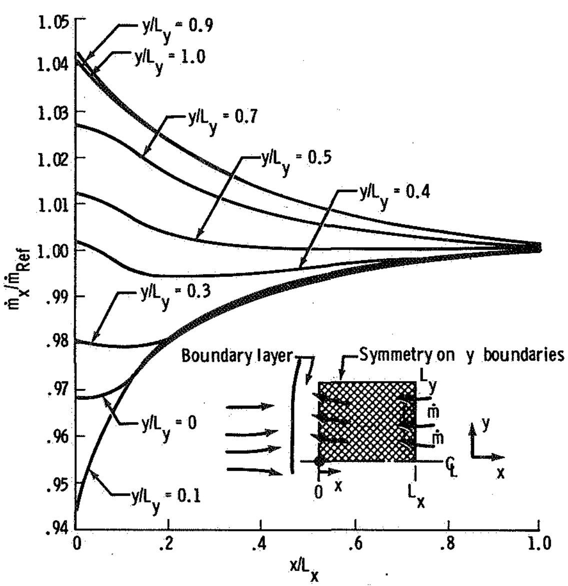

Figure 7. - Mass flux ratio normal to the surface for a two-dimensional, steady isothermal flow with the external pressure gradient (metallic matrix); where $P_{Stag} = 2.03 \times 10^{3}$ N/m^{2} and $\dot{m}_{Ref} = 110.3$ kg/m^{2}-hr.

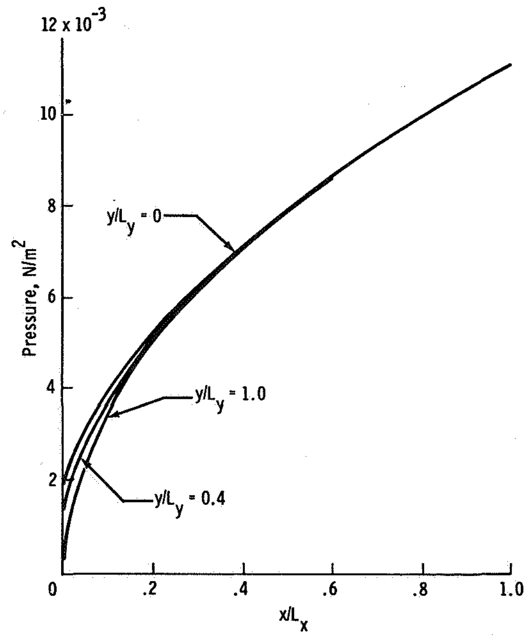

Figure 8. - Internal pressure distribution for a two-dimensional, steady isothermal flow with the external pressure gradient (metallic matrix); where $P_{Stag} = 2.03 \times 10^{3}$ N/m^{2} and $\dot{m}_{Ref} = 110.3$ kg/m^{2}-hr.

However, additional results with higher stagnation pressures show significant departure from one-dimensional flow within the porous matrix. For the case of an external stagnation pressure of 6.08×10^3 N/m^2, substantial variation in the mass flow-rate distribution (fig. 9) is in the stagnation region (small y/L_y). The corresponding internal pressure distribution is shown in figure 10.

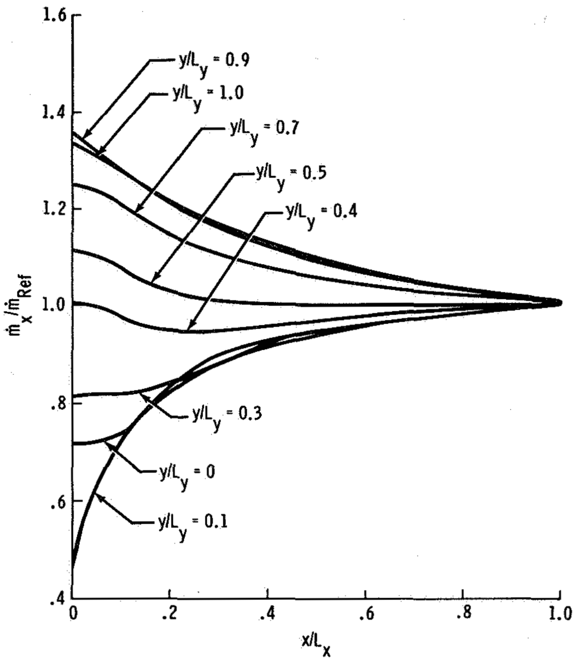

Figure 9.- Mass flux ratio normal to the surface for a two-dimensional, steady isothermal flow with the external pressure gradient (metallic matrix); where $P_{Stag} = 6.08 \times 10^3$ N/m^2 and $\dot{m}_{Ref} = 109.6$ kg/m^2-hr.

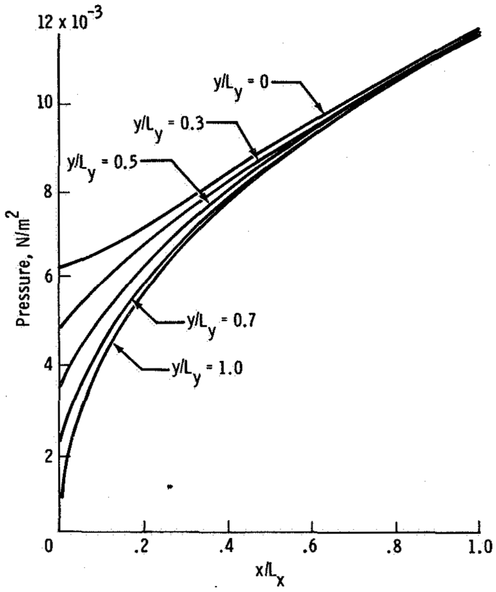

Figure 10.- Internal pressure distribution for a two-dimensional, steady isothermal flow with the external pressure gradient (metallic matrix); where $P_{Stag} = 6.08 \times 10^3$ N/m^2 and $\dot{m}_{Ref} = 109.6$ kg/m^2-hr.

Nonisothermal Solutions

For the nonisothermal case, the combined effects of a variable pressure and heat flux acting on the external surface $(0,y)$ and of a variable mass injection rate at the backface (L_x,y) are obtained by using the dimensionless distributions of figure 6. The coupled results shown in the following figures were obtained for the conditions of both thermal equilibrium and thermal nonequilibrium between the solid and fluid phases. In these nonisothermal considerations, a porous char matrix has been used. The thermophysical properties of the char material are shown in table I. All heat-transfer calculations are for a stagnation point heating rate of 567.5 kW/m^2 and an initial temperature of 556 K.

The temperature distribution has been nondimensionalized by using the equilibrium surface temperature. The effect of the variable external heat flux on the temperature distribution demonstrates the two-dimensional effects as indicated in figures 11 to 14. The temperature distributions shown in figures 11 and 12 were obtained by using a variable surface heat flux distribution with a constant mass injection rate at the rear boundary (L_x, y). The effect of the variable heat flux on the in-depth mass flux distribution (fig. 13) emphasizes the two-dimensional nature of the internal flow caused by in-depth pressure and density distributions. The internal pressure distribution is shown in figure 14.

TABLE I.- THERMOPHYSICAL PROPERTIES OF POROUS CHAR MATRIX

(a) Constant property values

Property	Value
Density, ρ, kg/m^3	320
Surface emissivity, ϵ	0.75
Porosity, ϕ	0.66
Viscous coefficient, α, m^{-2} . . .	6.22×10^{10}
Inertial coefficient, β, m^{-1} . . .	6.31×10^5

(b) Thermal conductivity k_s as a function of temperature

Temperature, K	k_s, W/m-K
256	0.00055
422	.00084
811	.00084
1033	.00175
1144	.00337
1478	.00597
1589	.00631
2172	.00914
2200	.00956
2367	.00956
2700	.00751
2783	.00685

(c) Specific heat C_{p_s} as a function of temperature

Temperature, K	C_{p_s}, J/kg-K
265	1549
811	1549
1367	1725
2756	1725
5033	1926

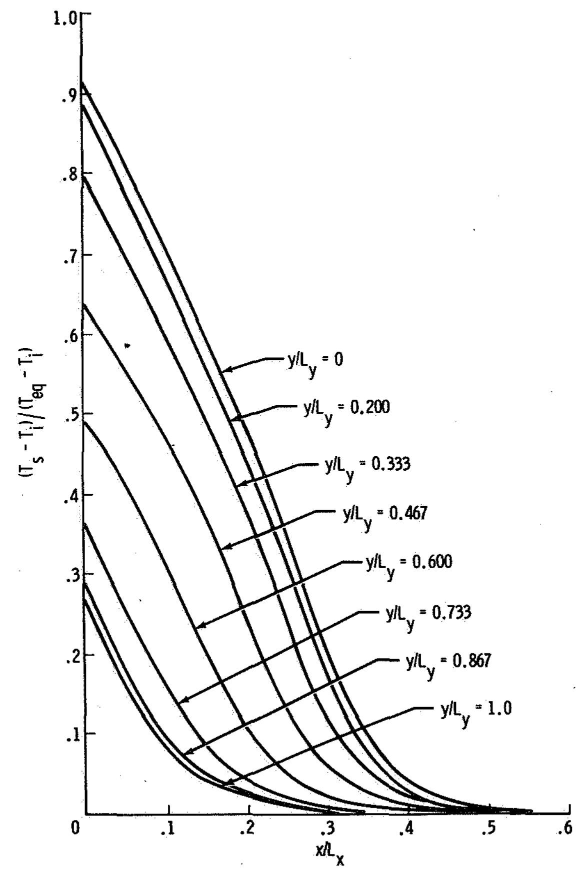

Figure 11.- Two-dimensional transient solid temperature distribution in char matrix (variable external heat flux); where $\dot{m}_{Ref} = 68.2$ kg/m^2-hr and t = 20 seconds.

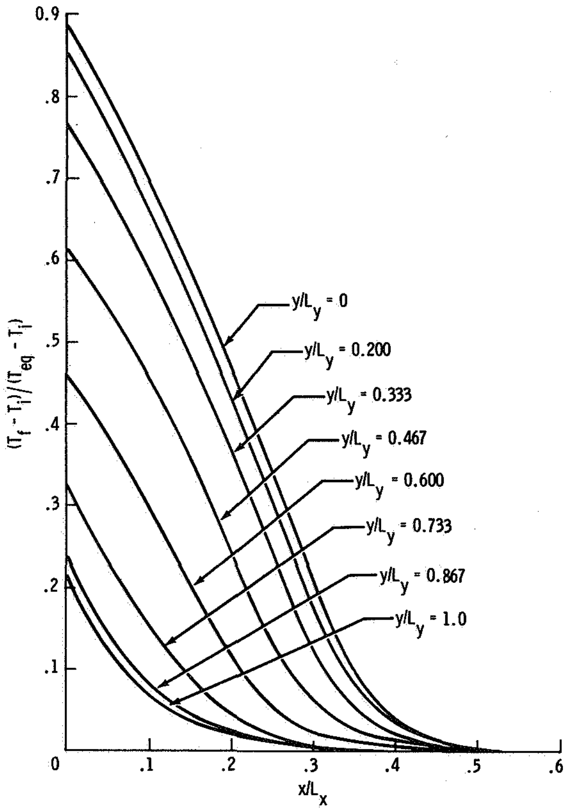

Figure 12.- Two-dimensional transient fluid temperature distribution in char matrix (variable external heat flux); where $\dot{m}_{Ref} = 68.2$ kg/m^2-hr and t = 20 seconds.

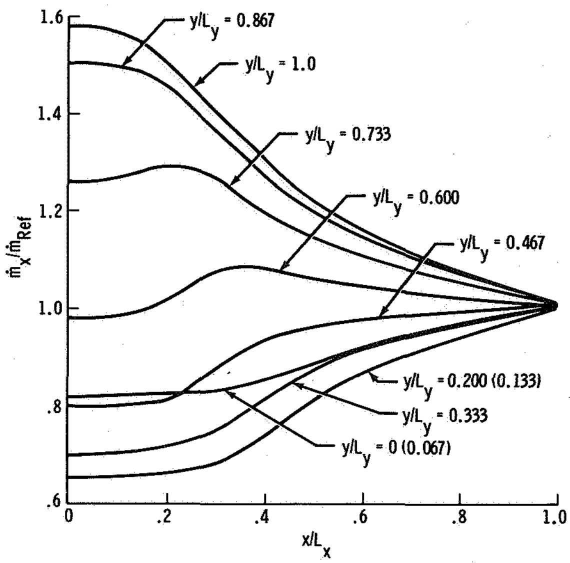

Figure 13.- Mass flux ratio normal to the surface for char matrix (variable external heat flux); where $T_{solid} \neq T_{fluid}$, $\dot{m}_{Ref} = 68.2$ kg/m^2-hr, and t = 20 seconds.

Figures 15, 16, and 17 provide the dimensionless temperature, mass flux, and pressure distribution, respectively, for the case of combined variable heat flux and pressure distributions together with a variable mass injection distribution at the rear boundary. The temperature distribution is very similar to that of figure 11. Once again, a pronounced two-dimensional in-depth flow was present; the mass flux ratio along a constant y/L_y line increased as the front surface was approached for $y/L_y > 0.6$ and $x/L_x < 0.6$. This, again, resulted from higher in-depth pressures associated with the stagnation region.

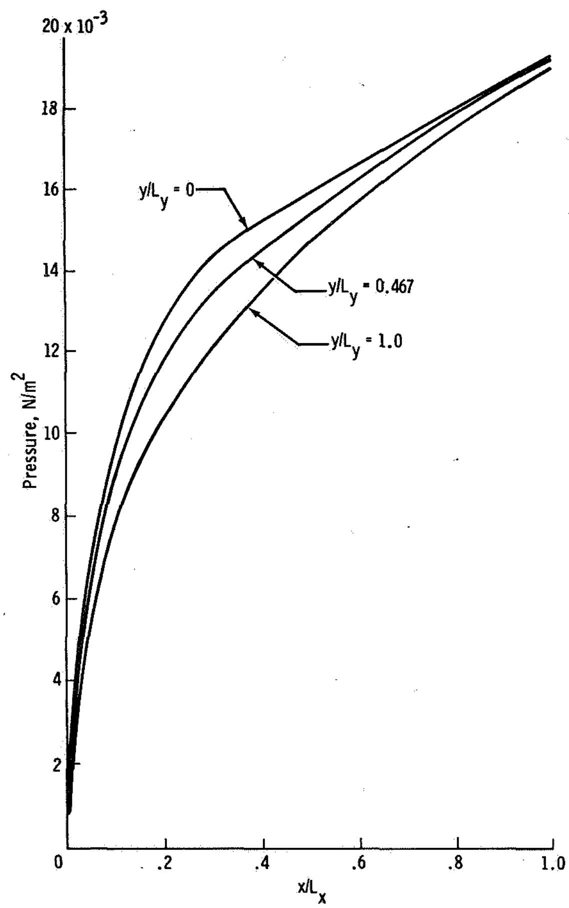

Figure 14. - Internal pressure distribution of char matrix (variable external heat flux); where $T_{solid} \neq T_{fluid}$, $\dot{m}_{Ref} = 68.2\ kg/m^2\text{-hr}$, and $t = 20$ seconds.

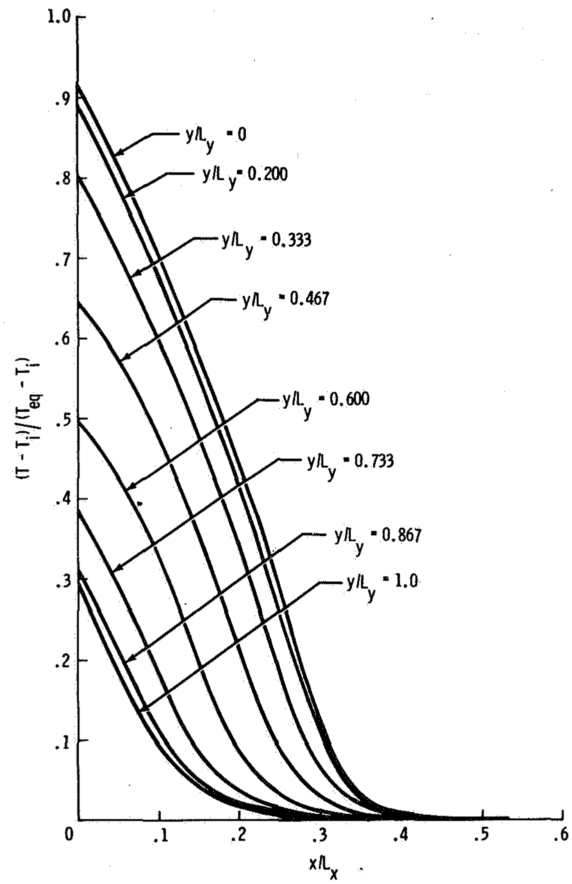

Figure 15. - Two-dimensional transient temperature distribution for char matrix assuming thermal equilibrium (variable heat flux, pressure, and mass injection); where $\dot{m}_{Ref} = 67\ kg/m^2\text{-hr}$, $P_{Stag} = 2.03 \times 10^3\ N/m^2$, and $t = 20$ seconds.

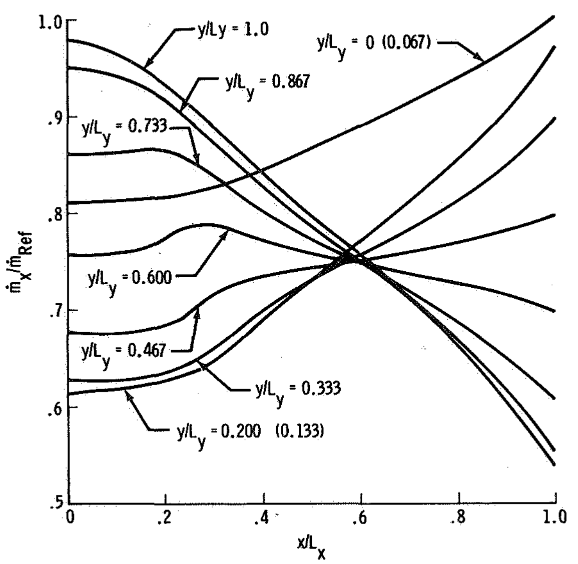

Figure 16. - Internal mass flux ratio normal to surface for char matrix (variable heat flux, pressure, and mass injection); where $\dot{m}_{Ref} = 67\ kg/m^2$-hr, $P_{Stag} = 2.03 \times 10^3\ N/m^2$, and t = 20 seconds.

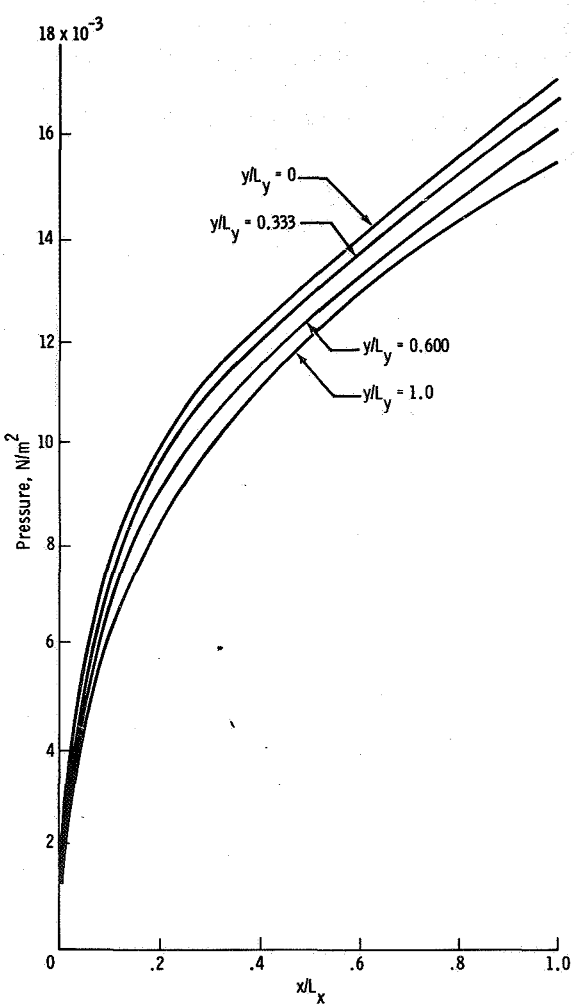

Figure 17. - Internal pressure distribution of char matrix (variable heat flux, pressure, and mass injection); where $\dot{m}_{Ref} = 67\ kg/m^2$-hr, $P_{Stag} = 2.03 \times 10^3\ N/m^2$, and t = 20 seconds.

CONCLUDING REMARKS

The flow of a compressible gas through a porous matrix externally heated at the fluid exit surface has been investigated. The physical model was formulated to simulate the flow of a pyrolysis gas formed during the degradation of an ablative material. The formulation of a numerical solution to the coupled energy, mass, and momentum relations describing this multidimensional flow of gas through a high-temperature porous matrix has been achieved. Two-dimensional coupled solutions were obtained using the strongly implicit procedure.

In this study, the strongly implicit procedure has been successfully applied to the solution of a system of coupled, nonlinear partial differential equations. The numerical results indicate the significance of multidimensional flow for both isothermal as well as nonisothermal effects in a porous material subjected to nonuniform boundary conditions.

Lyndon B. Johnson Space Center
National Aeronautics and Space Administration
Houston, Texas, January 11, 1974
986-15-31-04-72

APPENDIX A

DERIVATION OF THEORETICAL RELATIONS

The basic conservation relations for mass, energy, and momentum are applied to a compressible gas flowing through a high-temperature porous matrix. A continuum is assumed to exist in the porous matrix.

CONSERVATION OF MASS

The continuity equation for the unsteady flow of a single-species gas with a source term is

$$\phi \frac{\partial \rho}{\partial t} + \nabla \cdot \left(\rho_f \vec{V}_f\right) = m''' \tag{A1}$$

where the superficial fluid velocity $\vec{V}_f = \phi \vec{v}$ and $\vec{v}$ is velocity in a pore.

CONSERVATION OF MOMENTUM.

The conservation of momentum based on Newton's second law of motion is

$$\frac{\partial\left(\rho_f \vec{v}\right)}{\partial t} + \nabla \cdot \left(\rho_f \vec{v}\vec{v}\right) = -\nabla P - \nabla \cdot \tau + \rho_f g \tag{A2}$$

where τ is the viscous stress tensor and g is the gravitational constant. Direct application of this equation to flow in porous media has been discussed by Whitaker (ref. 12). The inability to specify exactly the flow geometry of the porous matrix and boundary conditions makes the solution of equation (A2) unfeasible.

The viscous force term $\nabla \cdot \tau$ was evaluated experimentally by Darcy (ref. 13) for slow, steady incompressible flow. These assumptions yield

$$\nabla P = \nabla \cdot \tau \tag{A3}$$

Darcy's results indicated that

$$\nabla \cdot \tau = \frac{\mu}{K} \vec{V} \tag{A4}$$

where K is the proportionality factor. Substituting equation (A4) into the constant-density flow form of equation (A2) yields

$$\frac{\rho_f}{\phi} \frac{d\vec{V}}{dt} = -\nabla P - \frac{\mu}{K} \vec{V} + \rho_f g \tag{A5}$$

Equation (A5) is known as the generalized Darcy Law (ref. 14). This equation contains both a viscous and an inertial contribution to the fluid motion. The substantial derivative of $\vec{V}$ contains both the temporal and the convective acceleration of the fluid. The basic assumption in this generalization of Darcy's Law is the use of equation (A4) as representative of the viscous stress tensor.

The validity of Darcy's Law for slow, viscous flow has been established. However, the use of this law at high-velocity flows does not correlate with experimental evidence. Equation (A6) correlates the experimental results of pressure drop and flow rates in a porous medium and has provided the necessary analytical correlation for predicting performance at other conditions (refs. 15 and 16).

$$-\nabla P = \left(\alpha \mu + \beta \rho_f \left|\vec{V}\right|\right)\vec{V} \tag{A6}$$

The term $\beta \rho_f \left|\vec{V}\right| \vec{V}$ in equation (A6) is basically comparable to the operation $\rho_f \vec{V} \cdot \nabla \vec{V}$ in equation (A5). This modified Darcy equation (eq. (A6)) is assumed valid for use as the conservation of momentum relation.

CONSERVATION OF ENERGY

The development of the energy equation follows the approach of Bird et al. (ref. 17) and Clark (ref. 18). The fluid energy equation can be written, neglecting radiation and gravity effects, as

$$\frac{\partial}{\partial t}\left[\rho\left(\hat{U} + \frac{1}{2} v^2\right)\right] + \left[\nabla \cdot \rho \vec{v}\left(\hat{U} + \frac{1}{2} v^2\right)\right] = \nabla \cdot \left(k_f \nabla T_f\right) - \left(\nabla \cdot P\vec{v}\right) - \left[\nabla \cdot \left(\tau \cdot \vec{v}\right)\right] + \frac{h_v}{\phi}\left(T_s - T_f\right) + q''' \tag{A7}$$

where $\hat{U}$ is the total internal energy. Equation (A8) is obtained by performing the indicated differentiations on the left side of equation (A7), applying the definition of the substantial derivative, and using the mechanical energy equation.

$$\rho \frac{d}{dt}(\hat{U}) + \left(\hat{U} + \frac{1}{2} v^2\right)\left[\frac{\partial \rho}{\partial t} + \nabla \cdot (\rho \vec{v})\right] = \nabla \cdot \left(k_f \nabla T_f\right) - P\left(\nabla \cdot \vec{v}\right) + \frac{h_v}{\phi}\left(T_s - T_f\right) + q''' + \Phi \tag{A8}$$

where Φ is viscous dissipation. Using the continuity equation (eq. (A1)) and the definition of enthalpy, equation (A8) may be written, neglecting viscous dissipation for a perfect gas, as

$$\rho_f C_{p_f} \frac{dT_f}{dt} - \frac{dP}{dt} + \left(C_{p_f} T_f + \frac{1}{2} v^2\right) m''' = \nabla \cdot \left(k_f \nabla T_f\right) + q''' + \frac{h_v}{\phi}\left(T_s - T_f\right) \tag{A9}$$

which is equation (2) in the text.

ENERGY EQUATION FOR SOLID

Application of the law of energy conservation to the solid state yields

$$\rho_s C_{p_s} \frac{\partial T_s}{\partial t} = \nabla \cdot \left(k_s \nabla T_s\right) - \frac{h_v}{(1 - \phi)}\left(T_s - T_f\right) + q''' \tag{A10}$$

which is equation (3) in the text.

REDUCTION OF GOVERNING EQUATIONS

The pressure, flow rate, and temperature distributions in a porous medium are obtained by a simultaneous solution of equations (A1), (A6), (A9), and (A10), in conjunction with an equation of state and the boundary and initial conditions. However, it is possible to reduce the number of equations by combining Darcy's Law and the continuity equation.

Assuming that the mass flux through the porous matrix can be regarded as constant for an iteration, equation (A6) can be solved explicitly for $\vec{V}$.

$$\vec{V} = \frac{-\nabla P}{\left(\alpha\mu + \beta\rho\left|\vec{V}\right|\right)} \tag{A11}$$

Now, using the perfect gas law

$$\rho = \frac{P}{RT_f} \tag{A12}$$

And substituting equations (A11) and (A12) into equation (A6) yields

$$\phi \frac{\partial}{\partial t}\left(\frac{P}{RT_f}\right) - \nabla \cdot \left[\frac{P \nabla P}{RT_f\left(\alpha\mu + \beta\rho\left|\vec{V}\right|\right)}\right] = m''' \tag{A13}$$

Noting that

$$\frac{\partial P}{\partial t} = \frac{1}{2P} \frac{\partial P^2}{\partial t} \tag{A14}$$

and

$$\nabla \cdot (P \nabla P) = \nabla \cdot \left(\frac{\nabla P^2}{2}\right) \tag{A15}$$

yields

$$\frac{\phi}{P} \frac{\partial}{\partial t}\left(\frac{P^2}{T_f}\right) - \nabla \cdot \left[\frac{\nabla P^2}{T_f\left(\alpha\mu + \beta\rho\left|\vec{V}\right|\right)}\right] = 2Rm''' \tag{A16}$$

This is the Darcy continuity equation (eq. (1)).

APPENDIX B

FINITE DIFFERENCE RELATIONS USING THE STRONGLY IMPLICIT TECHNIQUE

The fluid energy equation (eq. (2)) is put in finite difference form as an illustration of its application to the strongly implicit procedure (SIP) algorithm. The same procedure was followed for the Darcy continuity and solid energy equations.

INTERIOR NODES

Assuming for illustration purposes that $m''' = 0$, $q''' = 0$, and $dP/dt = 0$, equation (2) can be written

$$C_{p_f}\rho_f\left(\frac{\partial T_f}{\partial t} + u\frac{\partial T_f}{\partial x} + v\frac{\partial T_f}{\partial y}\right) = \frac{\partial}{\partial x}\left(k_f\frac{\partial T_f}{\partial x}\right) + \frac{\partial}{\partial y}\left(k_f\frac{\partial T_f}{\partial y}\right) + \frac{h_v}{\phi}\left(T_s - T_f\right) \qquad \text{(B1)}$$

Using central differences and spatially averaged thermal conductivities, equation (B1) can be written as

$$\begin{aligned}
&\frac{T'_{f_{i,j}} - T_{f_{i,j}}}{\Delta t} - u_{i,j}\left(\frac{T'_{f_{i+1,j}} - T'_{f_{i-1,j}}}{2\Delta x}\right) \\
&+ v_{i,j}\left(\frac{T'_{f_{i,j+1}} - T'_{f_{i,j-1}}}{2\Delta y}\right) = \left[\frac{AX_{i+1,j} + AX_{i,j}}{(\Delta x)^2}\right]T'_{f_{i+1,j}} \\
&- \left[\frac{AX_{i+1,j} + AX_{i,j}}{2(\Delta x)^2} + \frac{AX_{i,j} + AX_{i-1,j}}{2(\Delta x)^2} + \frac{AY_{i,j+1} + AY_{i,j}}{2(\Delta y)^2}\right. \\
&\left. + \frac{AY_{i,j-1} + AY_{i,j}}{2(\Delta y)^2}\right]T'_{f_{i,j}} + \left[\frac{AX_{i-1,j} + AX_{i,j}}{2(\Delta x)^2}\right]T'_{f_{i-1,j}} \\
&+ \left[\frac{AY_{i,j+1} + AY_{i,j}}{2(\Delta y)^2}\right]T'_{f_{i,j+1}} + \left[\frac{AY_{i,j} + AY_{i,j-1}}{2(\Delta y)^2}\right]T'_{f_{i,j-1}} \\
&- \frac{h_{v_i}}{\phi\rho_{f_i}C_{p_i}}T'_{f_{i,j}} + \frac{h_{v_i}}{\phi\rho_{f_i}C_{p_i}}T_{s_{i,j}}
\end{aligned} \qquad \text{(B2)}$$

where

$$AX = \frac{k_{fx}}{\rho_f C_{p_f}} \quad \text{and} \quad AY = \frac{k_{fy}}{\rho_f C_{p_f}} \tag{B3}$$

Formulating equation (B2) as

$$AT'_{i,j-1} + BT'_{i-1,j} + CT'_{i,j} + DT'_{i+1,j} + ET'_{i,j+1} = Q_{i,j} \tag{B4}$$

(which is equation (16)) requires that

$$A_{i,j} = \frac{v_{i,j}}{2\Delta y} + \frac{AY_{i,j} + AY_{i,j-1}}{2(\Delta y)^2} \tag{B5a}$$

$$B_{i,j} = -\frac{u_{i,j}}{2\Delta x} + \frac{AX_{i-1,j} + AX_{i,j}}{2(\Delta x)^2} \tag{B5b}$$

$$C_{i,j} = -\left[\frac{1}{\Delta t} + \frac{AX_{i+1,j} + AX_{i,j}}{2(\Delta x)^2} + \frac{AX_{i-1,j} + AX_{i,j}}{2(\Delta x)^2}\right.$$

$$\left. + \frac{AY_{i,j} + AY_{i,j+1}}{2(\Delta y)^2} + \frac{AY_{i,j} + AY_{i,j-1}}{2(\Delta y)^2} + \frac{h_{v_i}}{\phi\rho_{f_i} C_{p_{f_i}}}\right] \tag{B5c}$$

$$D_{i,j} = \frac{AX_{i+1,j} + AX_{i,j}}{2(\Delta x)^2} + \frac{u_{i,j}}{2\Delta x} \tag{B5d}$$

$$E_{i,j} = \frac{AY_{i,j} + AY_{i,j+1}}{2(\Delta y)^2} - \frac{v_{i,j}}{2\Delta y} \tag{B5e}$$

$$Q_{i,j} = -\frac{T_{f_{i,j}}}{\Delta t} - \left(\frac{h_{v_{i,j}}}{\phi\rho_{f_i} C_{p_{f_i}}} T_{s_{i,j}}\right) \tag{B5f}$$

BOUNDARY CONDITIONS

As an illustration of the boundary condition requirements, consider the heated surface at $x = 0$, $y = 0$ (fig. 4). The SIP boundary restrictions require $A = B = 0$. Therefore, equation (B4) becomes

$$CT'_{i,j} + DT'_{i+1,j} + ET'_{i,j+1} = Q_{i,j} \tag{B6}$$

where the boundary conditions

$$\frac{\partial T_f}{\partial y} = 0 \quad \text{or} \quad T'_{i,j-1} = T'_{i,j+1} \tag{B7}$$

and

$$\frac{\partial^2 T_f}{\partial x^2} = 0 \tag{B8}$$

have been used.

REFERENCES

1. Curry, Donald M.; and Stephens, Emily W.: Apollo Ablator Thermal Performance at Superorbital Entry. NASA TN D-5969, 1970.

2. Bush, Harold G.; and Dow, Marvin B.: Multidimensional Gas Flow Through Permeable Char Layers and Its Effects on Ablation. NASA TR R-296, 1969.

3. Bland, D. R.: Mathematical Theory of the Flow of a Gas in a Porous Solid and of the Associated Temperature Distributions. Proc. Roy. Soc. (London), A, 221, 1954, pp. 1-28.

4. Schneider, P. J.; Mauer, R. E.; and Strapp, M. G.: Two-Dimensional Transpiration Cooling. AIAA Paper No. 69-96, 1969.

5. Del Casal, E. P.: The Effects of Multidimensional Flow Through Porous Matrices in Mass Transfer Cooling. AIAA Paper No. 69-149, 1969.

6. Pittman, Claud M.; and Howser, Lona M.: Numerical Analysis of the Transient Response of an Axisymmetric Ablative Char Layer Considering Internal Flow Effects. NASA TN D-6895, 1972.

7. Peaceman, D. W.; and Rachford, H. W.: The Numerical Solution of Parabolic and Elliptic Differential Equations. J. Soc. Ind. Appl. Math., vol. 3, 1955, pp. 28-41.

8. Stone, Herbert L.: Iterative Solution of Implicit Approximations of Multidimensional Partial Differential Equations. SIAM J. Numerical Analysis, vol. 5, no. 3, Sept. 1968, pp. 530-558.

9. Bozeman, J. D.: Numerical Solutions for Recirculating Flow in a Cavity. Ph. D. Dissertation, Univ. of Houston, 1971.

10. Curry, Donald Morgan: Multi-Dimensional Analysis of Heat and Mass Transfer in Porous Media. Ph. D. Dissertation, Univ. of Houston, 1970.

11. Kreith, Frank: Principles of Heat Transfer. International Textbook Co., 1958, p. 535.

12. Whitaker, S.: The Equations of Motion in Porous Media. Chem. Eng. Sci., vol. 21, Mar. 1966, pp. 291-300.

13. Darcy, H.: Les Fontaines Publiques de la Ville de Dijon. 1856.

14. Yih, Chia-shun: Dynamics of Nonhomogeneous Fluids. Macmillan, 1965, pp. 196-199.

15. Green, Leon, Jr.; and Duwez, Pol: Fluid Flow Through Porous Metals. J. Appl. Mech., vol. 18, Mar. 1951, pp. 39-45.

16. Greenberg, D. B.; and Weger, E.: An Investigation of the Viscous and Inertial Coefficients for the Flow of Gases Through Porous Sintered Metals with High Pressure Gradients. Chem. Eng. Sci., vol. 12, no. 1, 1960, pp. 8-19.

17. Bird, Robert Byron; Stewart, Warren E.; and Lightfoot, Edwin N.: Transport Phenomena. John Wiley & Sons, Inc., 1964.

18. Clark, R. K.: Flow of Hydrocarbon Gases in Porous Media at Elevated Temperatures. M. S. Thesis, Univ. of Virginia, 1968.

NATIONAL AERONAUTICS AND SPACE ADMINISTRATION
WASHINGTON, D.C. 20546

OFFICIAL BUSINESS
PENALTY FOR PRIVATE USE $300

SPECIAL FOURTH-CLASS RATE
BOOK

POSTAGE AND FEES PAID
NATIONAL AERONAUTICS AND
SPACE ADMINISTRATION
451

U.S.MAIL

POSTMASTER: If Undeliverable (Section 158 Postal Manual) Do Not Return

---

"The aeronautical and space activities of the United States shall be conducted so as to contribute . . . to the expansion of human knowledge of phenomena in the atmosphere and space. The Administration shall provide for the widest practicable and appropriate dissemination of information concerning its activities and the results thereof."

—NATIONAL AERONAUTICS AND SPACE ACT OF 1958

NASA SCIENTIFIC AND TECHNICAL PUBLICATIONS

TECHNICAL REPORTS: Scientific and technical information considered important, complete, and a lasting contribution to existing knowledge.

TECHNICAL NOTES: Information less broad in scope but nevertheless of importance as a contribution to existing knowledge.

TECHNICAL MEMORANDUMS: Information receiving limited distribution because of preliminary data, security classification, or other reasons. Also includes conference proceedings with either limited or unlimited distribution.

CONTRACTOR REPORTS: Scientific and technical information generated under a NASA contract or grant and considered an important contribution to existing knowledge.

TECHNICAL TRANSLATIONS: Information published in a foreign language considered to merit NASA distribution in English.

SPECIAL PUBLICATIONS: Information derived from or of value to NASA activities. Publications include final reports of major projects, monographs, data compilations, handbooks, sourcebooks, and special bibliographies.

TECHNOLOGY UTILIZATION PUBLICATIONS: Information on technology used by NASA that may be of particular interest in commercial and other non-aerospace applications. Publications include Tech Briefs, Technology Utilization Reports and Technology Surveys.

Details on the availability of these publications may be obtained from:

SCIENTIFIC AND TECHNICAL INFORMATION OFFICE

NATIONAL AERONAUTICS AND SPACE ADMINISTRATION

Washington, D.C. 20546